Size control of the *Drosophila* hematopoietic niche by bone morphogenetic protein signaling reveals parallels with mammals

Delphine Pennetier[a], Justine Oyallon[a], Ismaël Morin-Poulard[a], Sébastien Dejean[b], Alain Vincent[a,1], and Michèle Crozatier[a,1]

[a]Centre de Biologie du Développement, Unité Mixte de Recherche 5547 Centre National de la Recherche Scientifique/Université Toulouse III and Fédération de Recherche de Biologie de Toulouse, 31062 Toulouse Cedex 9 France; and [b]Institut de Mathématiques, Université Toulouse III, 31062 Toulouse Cedex 9 France

Edited by Utpal Banerjee, University of California, Los Angeles, CA 90095-7239, and accepted by the Editorial Board January 23, 2012 (received for review June 10, 2011)

The *Drosophila melanogaster* larval hematopoietic organ, the lymph gland, is a model to study in vivo the function of the hematopoietic niche. A small cluster of cells in the lymph gland, the posterior signaling center (PSC), maintains the balance between hematopoietic progenitors (prohemocytes) and their differentiation into specialized blood cells (hemocytes). Here, we show that Decapentaplegic/bone morphogenetic protein (Dpp/BMP) signaling activity in PSC cells controls niche size. In the absence of BMP signaling, the number of PSC cells increases. Correlatively, no hemocytes differentiate. Controlling PSC size is, thus, essential for normal blood cell homeostasis. Activation of BMP signaling in the PSC requires expression of the Dally-like heparan-sulfate proteoglycan, under the control of the Collier/early B-cell factor (EBF) transcription factor. A Dpp > dpp autoregulatory loop maintains BMP signaling, which limits PSC cell proliferation by repressing the protooncogene *dmyc*. Dpp antagonizes activity of wingless (Wg)/Wnt signaling, which positively regulates the number of PSC cells via the control of Dmyc expression. Together, our data show that Collier controls hemocyte homeostasis via coordinate regulation of PSC cell number and PSC signaling to prohemocytes. In mouse, EBF2, BMP, and Wnt signaling in osteoblasts is required for the proper number of niche and hematopoietic stem cells. Our findings bring insights to niche size control and draw parallels between *Drosophila* and mammalian hematopoiesis.

TGF-β | hematopoiesis | myc

Larval hematopoiesis in *Drosophila* takes place in a specialized organ, the lymph gland (LG), composed of paired lobes positioned along the aorta (1–3). The anterior/primary lobes of the mature LG are organized into a medullary zone (MZ) containing prohemocytes; a cortical zone (CZ) containing two types of differentiated hemocytes, plasmatocytes and crystal cells, as well as intermediate progenitors; and the posterior signaling center (PSC) (Fig. 1*Q*) (3–5). PSC cells are specified in the embryo by two transcription factors, the Hox protein Antennapedia (Antp) and Collier (Col) (6–8). Signals issued from the PSC, such as Hedgehog (Hh), act in a non-cell-autonomous manner to maintain the activities of Hh and JAK-STAT signaling pathways in the MZ, thereby preserving a pool of multipotent progenitors throughout larval development (7, 8). This role of the PSC in controlling *Drosophila* blood cell homeostasis revealed unanticipated parallels with the hematopoietic stem cell (HSC) niche in the mammalian bone marrow (7–9). In mammals, the size of the HSC niche is tightly regulated to maintain HSCs and normal homeostasis (10, 11). PSC cells account for ∼15% of the total LG cells at the end of embryogenesis but only ∼1% in mid-third-instar (mid-L3) larvae, when hemocyte differentiation occurs (3), indicating that proliferation of PSC cells is tightly controlled (5). Although loss- and gain-of-function experiments have established that Antp activity and Wg/Wnt signaling positively regulate the proliferation of PSC cells (7, 12), how their number is kept low throughout larval development remains unknown. *Drosophila* Decapentaplegic (Dpp), a member of the transforming growth factor (TGF)-β family is well known for its role in controlling proliferation in imaginal tissues and maintaining germline stem cells in the ovary (10, 13–16). Likewise, BMP4 was shown recently to be expressed and regulate the mouse HSC (17). Here, we addressed the role of BMP signaling in the *Drosophila* LG.

Results and Discussion

BMP Signaling in the PSC Controls the Niche Size. TGF-β/BMP/Dpp signaling in *Drosophila* acts through two branches, the BMP and activin pathways, and is initiated by TGFβ ligand binding to a type II receptor, which recruits and phosphorylates a type I receptor. The type I receptor then phosphorylates a transcription factor of the receptor-regulated SMAD (R-SMAD) family, allowing its interaction with a co-Smad and accumulation in the nucleus, where it regulates target gene expression (18). For BMP signaling, there are three TGF-β family ligands, Dpp, Glass bottom boat (Gbb), and Screw (Scw); two type I receptors, Thickveins (Tkv) and Saxophone (Sax); two type II receptors, Wishful thinking (Wit) and Punt; one Smad transcription factor, Mother against Dpp (Mad); and one cofactor, Medea (18). Daughters against dpp (Dad), a direct target gene of Dpp signaling, acts in a negative-feedback loop. Activity of the BMP signaling pathway can be detected by the presence of phosphorylated (P)-Mad and the expression of a dad-GFP transgene (19–22). We found that both high level dad-GFP expression and P-Mad accumulation were restricted to PSC cells in wt LGs (Fig. 1 *A*–*C*′), establishing that BMP signaling is specifically activated in the niche. To address the role of this signaling, we used a col-Gal4 driver (8) and expressed a dominant-negative form of the type I receptor Tkv (Tkv^{DN}) in the PSC and, at the same time, a membrane-bound form of GFP to visualize PSC cells (col > GFP > tkv^{DN}) (8). In this and all subsequent experiments, and unless otherwise stated, we used mid-L3 larvae [96 h after egg laying (AEL)] for LG analyses. Blocking Dpp signaling resulted in a fourfold increase in the number of PSC cells (Fig. 1 *D* and *F*), showing that the BMP pathway negatively regulates the PSC size. To identify which BMP receptors and ligands act in the PSC, we tested different mutants. The average number of PSC cells was increased from 20 in wt to 80 in col > tkv^{DN}, 65 in *wit* and 50 cells in *tkv*, and *dpp* mutants, respectively (Fig. 1*F* and Fig. S1), whereas

Author contributions: D.P., J.O., I.M.-P., A.V., and M.C. designed research; D.P., J.O., I.M.-P., and M.C. performed research; D.P., J.O., I.M.-P., S.D., A.V., and M.C. analyzed data; and A.V. and M.C. wrote the paper.

The authors declare no conflict of interest.

This article is a PNAS Direct Submission. U.B. is a guest editor invited by the Editorial Board.

[1]To whom correspondence may be addressed. E-mail: alain.vincent@univ-tlse3.fr or crozat@cict.fr.

This article contains supporting information online at www.pnas.org/lookup/suppl/doi:10.1073/pnas.1109407109/-/DCSupplemental.

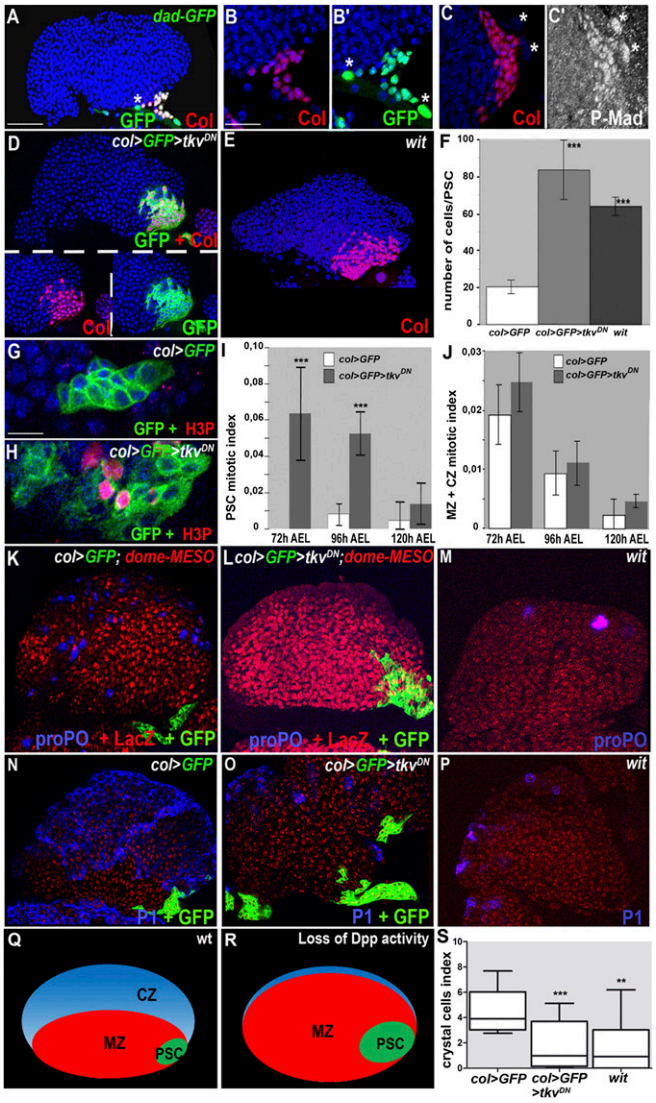

Fig. 1. The BMP signaling pathway is specifically activated in PSC cells and is required to limit their numbers. (*A*) dad-GFP expression (green) in the LG is restricted to PSC cells, marked by Col (red). (*B–C′*) Enlarged views showing colocalization of Col with dad-GFP (*B* and *B′*) and high P-Mad levels (*C* and *C′*); *pericardial cells. (*A–E*) Col staining (red) shows that the PSC of *col > GFP> tkv*^{DN} (*D*) and *wit* mutant larvae (*E*) contains roughly fourfold more cells than wt (*A* and *F*). (*G* and *H*) H3P staining (red) in the PSC (green) in the presence or absence of BMP signaling. (*I* and *J*) Measured mitotic indices of the PSC (*I*) and MZ + CZ (*J*), in wt and *col > GFP > tkv*^{DN} LGs, 72, 96, and 120 h AEL. Error bars represent SDs. ***$P < 0.001$ in *F* and *I* (Student *t* test). (*K–P*) *col > GFP* (*K* and *N*) and *col > GFP > tkv*^{DN} (*L* and *O*) LGs expressing *dome-MESO* in prohemocytes (red) and *wit* mutant LGs (*M* and *P*) stained for crystal cells (proPO; blue) (*K–M*) or plasmatocytes (P1; blue) (*N–P*). (*Q*) Schematic diagram of a wt LG lobe, with the PSC in green, MZ in red, and CZ containing intermediate progenitors and differentiated hemocytes in blue. (*R*) Loss of Dpp activity results in a bigger PSC and reduced levels of hemocyte differentiation. (*S*) Crystal cell index (***$P < 0.0009$; **$P < 0.0053$; *$P < 0.0147$). Nuclei are labeled by Topro (blue) (*A–E*, *G*, and *H*) and (red) (*M–P*). [Scale bars: 80 μm (*A*, *D*, *E*, *K–P*); 40 μm (*G* and *H*); 20 μm (*B–C′*).]

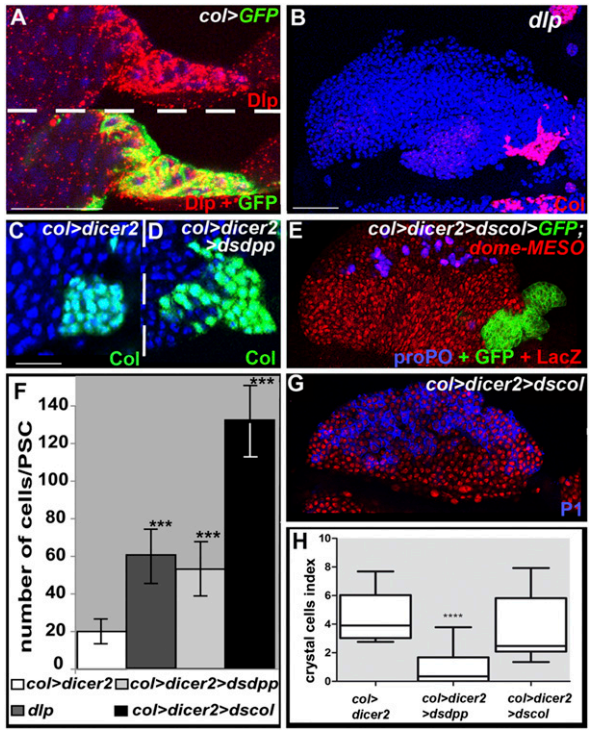

Fig. 2. BMP signaling in the PSC requires expression of Dally like under the control of Col and an autoregulatory loop. (*A*) Immunostaining of *col > GFP* LGs for Dlp (red), showing high level expression in PSC cells (green). (*B*) *dlp* mutant LGs display a larger PSC (Col immunostaining, pink). (*C* and *D*) Reducing *dpp* expression in the PSC leads to an increased number of PSC cells (*D*). (*E* and *G*) Decreasing *col* level in the PSC leads to an oversized PSC without affecting the balance between prohemocytes (dome-MESO expression, red) and either crystal cells (proPO, blue) (*E*) or plasmatocytes (P1, blue) (*G*). (*F*) Number of PSC cells (***$P < 0.001$; Student *t* test). (*H*) Crystal cell index (****$P < 0,0001$; Student *t* test). (Topro blue, *B–D*; red, *G*.) [Scale bars: 80 μm (*B*, *E*, and *G*); 40 μm (*A*, *C*, and *D*).]

no change was observed in either *punt* or *gbb* mutants (Fig. S1). Thus, BMP activation in PSC cells is mediated by Dpp binding to the Tkv/Wit receptors. Consistent with the fact that the *dpp* and *tkv* alleles allowing survival until the third instar are hypomorphs, a more robust increase in PSC cell numbers was observed upon Tkv^{DN} expression and in *wit*-null mutants. For this reason, we used col > GFP > tkv^{DN} for most of our analysis. Of note, a previous study, based on a hypomorphic *dpp* allele (*cis*-regulatory mutant), showed that impaired BMP signaling in the entire embryo resulted in a bigger embryonic LG, a phenotype persisting into third instar, although without significant difference in the number of Antp-expressing niche cells or differentiating crystal cells (23). The discrepancy between our present results and this initial report could be explained by the use of different alleles and different timing and targeting of *dpp* removal in the PSC.

Controlling the Niche Size Is Essential for Blood Cell Homeostasis in the Lymph Gland. Because PSC cells are lineage-segregated from the rest of the LG cells in embryos (5–7), the oversized PSC in the absence of BMP signaling suggested a change in proliferation intrinsic to these cells. We, therefore, compared the mitotic index of wt and col > tkv^{DN} LGs, using anti-phospho-histone H3 (H3P) antibody staining. The mitotic index of PSC cells from larvae dissected either 72 h AEL (early L3), 96 h AEL (mid-L3), or 120 h AEL (late L3) showed more divisions in the absence of BMP signaling (Fig. 1 *G–I*). This was particularly striking at 72 h AEL (Fig. 1 *G–I*). The mitotic index of the rest of the LG was not changed statistically significantly when Dpp signaling was switched off in the PSC, indicating that the increased number of PSC cells does not impact on the proliferation rate of prohemocytes (Fig. 1*J*). We concluded that BMP signaling specifically controls the proliferation of PSC cells. We then asked whether an increased number of niche cells affects the balance between prohemocytes and hemocytes in the LG. Prohemocytes can be identified by the expression of dome-MESO, a reporter of JAK-STAT signaling, whereas differentiated crystal cells and

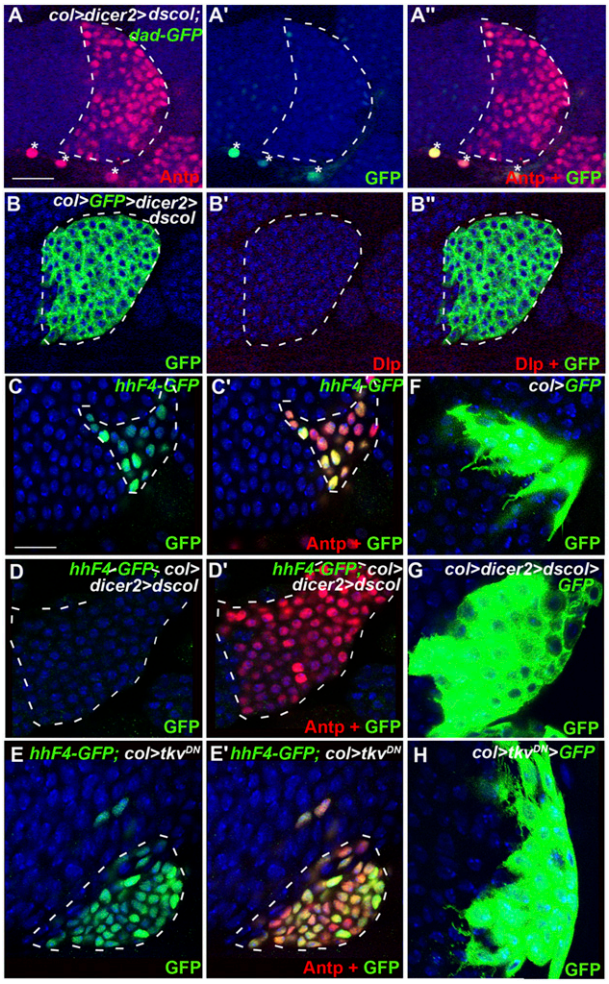

Fig. 3. Col expression in PSC cells is required for maintaining their signaling properties. (*A*–*A*′′) Double staining of *col* > *dscol* LGs for Antp (red) and dad-GFP (green). The PSC does not activate Dpp signaling upon removal of Col; *cardial cells. (*B*–*B*′′) Dlp expression (red) is also lost. (*C*–*E*′) Antp (red) and hh-GFP staining (green) labeling of PSC cells in wt (*C* and *C*′), *col* > *dicer2* > *dscol* (*D* and *D*′), and *col* > tkv^{DN} (*E* and *E*′) LGs. (*F*) PSC-targeted expression of mCD8-GFP (*col* > *mCD8-GFP*) shows numerous filopodia extended by wt PSC cells. (*G* and *H*) Filopodia are lost in the absence of Col activity (*G*), whereas they are preserved in the absence of Dpp activity (*H*). (Topro (blue), *A*–*H*.) [Scale bars: 40 μm (*A*–*B*′′); 20 μm (*C*–*H*).]

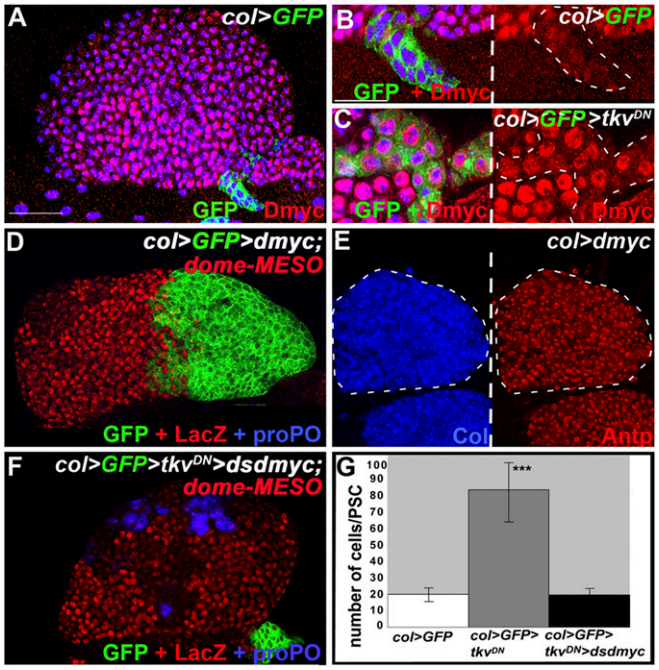

Fig. 4. PSC repression of the protooncogene *dmyc* by Dpp signaling. (*A* and *B*) Dmyc immunostaining (red) in wt LG. (*B*) Enlargement view showing that *col* > *GFP* PSC cells (green) express a very low level of Dmyc. (*C*) Inactivation of Dpp signaling (*col* > tkv^{DN}) in the PSC leads to increased Dmyc expression. (*D* and *E*) Overexpression of *dmyc* results in a very large PSC, visualized by either *col* > *GFP* (green) (*D*) or Col (blue) or Antp (red) (*E*). (*D*) dome-MESO expression (red) shows an expanded MZ, whereas no crystal cells (proPO, blue) differentiate. (*F* and *G*) PSC cell number is close to wt and hemocyte differentiation is restored (proPO staining, blue) when *dmyc* dsRNA and Tkv^{DN} are coexpressed in the PSC (green). ***$P < 0.001$ in *G* (Student *t* test). (Topro (blue) in *A*–*C*.) [Scale bars: 80 μm (*A*, *D*–*F*); 20 μm (*B*–*C*′).

plasmatocytes can be identified by anti-proPO and P1 antibody staining, respectively (8, 24). In contrast to wt mid-L3 LGs (3), differentiated crystal cells and plasmatocytes were rarely detected in either col > tkv^{DN} (Fig. 1 *K*, *L*, *N*, *O*, and *S*) or *wit*-null mutant (Fig. 1 *K*, *M*, *N*, *P*, and *S*) LGs, where the number of PSC cells is increased more than threefold (Fig. 1*F*). Most col > tkv^{DN} LG cells remained dome-MESO-positive, indicating that they were maintained as prohemocytes. Crystal cell and plasmatocyte differentiation was observed, however, in hypomorphic *dpp* or *tkv* mutants, where the number of PSC cells was around twofold the wt number (Fig. S1). Systematic quantification of crystal cells indicates that the balance between prohemocytes and differentiated hemocytes is tightly linked to PSC cell numbers and that controlling the size of the PSC is essential to control hemocyte homeostasis (7, 8, 12) (Fig. 1 *Q* and *R*).

BMP Signaling in the PSC Depends upon the HSPG Dally-Like and a BMP Autoregulatory Loop. In situ hybridization showed that *dpp*, *tkv*, and *wit* are ubiquitously expressed in LGs, indicating that transcriptional regulation of these three genes does not account for the restriction of BMP activity to PSC cells (Fig. S3). Specific localization of *dpp* transcript in the LG has been technically challenging. To determine which cells contribute to provide the source of Dpp that activates the BMP pathway in the PSC, we specifically reduced *dpp* transcripts in either the MZ or the PSC, by targeted expression of *dpp* double-stranded (ds)RNA. Whereas *dpp* depletion in the MZ (dome > dsdpp) had no effect on the size of the PSC, depletion in the PSC (col > dsdpp) led to an abnormally large PSC containing 55 cells on average, compared with 20 cells in wt (Fig. 2 *C*, *D*, and *F*), mimicking the *dpp* loss-of-function phenotype (Fig. 2*H* and Fig. S1). This indicates that the Dpp source responsible for active BMP signaling in the PSC is the PSC cells themselves. The absence of *dpp* transcripts in col > tkv^{DN} PSC cells further showed that BMP signaling controls *dpp* transcription (Fig. S3) through a Dpp > dpp positive-feedback regulatory loop, suggesting an autocrine and/or paracrine signaling mode in PSC cells (Fig. 6). Previous studies in other tissues have shown that Dally and Dally-like (Dlp), two glycosylphosphatidylinositol (GPI)-anchored heparan-sulfate proteoglycans (HSPGs), regulate Dpp activity in signal-transducing cells, in a cell-autonomous manner (25–29). Transcriptome analyses of LGs suggested that *dlp* is expressed in the PSC. Staining for the Dlp protein confirmed that it is expressed at high levels in PSC cells (Fig. 2 *A*). We, therefore, assayed the phenotype of *dlp* mutant larvae and found that they display both a strong decrease in P-Mad accumulation and increase in PSC cell number (Fig. 2 *B* and *F* and Fig. S2). This indicates that expression of Dlp in the PSC is required for high levels of BMP signaling in the PSC. Normal levels of Dlp expression are detected in col > tkv^{DN} PSC cells, indicating that Dlp expression

DEVELOPMENTAL BIOLOGY

is independent of Dpp activity (Fig. S3). Of note, in many tissues, a tight control of Dpp signaling is achieved, which involves different types of repressors (18, 30). How the BMP pathway is regulated in the LG, outside the PSC, requires additional investigation.

Collier/Early B-Cell Factor Controls Larval Hematopoiesis via BMP-Dependent and BMP-Independent Mechanisms. Col is expressed at a high level in the PSC, from the end of embryogenesis throughout larval development. Col requirement for specifying PSC cells in late embryos/early larvae, however, prevents assessing its role in the larva. To access *col* function in third-instar larvae, we used PSC-targeted expression of *col* dsRNA (col > coldsRNA > GFP). Col dsRNA expression reproduces *col* loss-of-function phenotypes in different tissues (31, 32). In these conditions, and unlike in *col*-null mutants, PSC cells are specified, likely reflecting the delay in the accumulation of col dsRNA that is introduced by the Gal4 system. Col > GFP expression and Antp immunostaining confirmed the maintenance of PSC cells (Figs. 2*E* and 3*A*). However, the number of PSC cells was approximately six times higher than in wt (Fig. 2 *E* and *F*), showing that *col* activity in larvae is required to maintain low PSC cell proliferation. The concomitant loss of dad-GFP expression in the PSC showed that the BMP pathway was inactive. Furthermore, Dlp was not detected in the PSC of col > coldsRNA LGs (Fig. 3 *B*–*B*′′). Together, the *col*, *dlp*, and *dpp* loss-of function phenotypes show that Col activity in the PSC controls the number of PSC cells via activation of Dlp expression and BMP signaling activity (Fig. 6). Surprisingly, the increased number of PSC cells upon col > coldsRNA expression did not prevent differentiation of crystal cells and plasmatocytes (Fig. 2 *E*, *G*, and *H*), unlike the observation in col > tkv^{DN} LGs. This suggests that, in absence of Col activity at larval stages, PSC cells overproliferate but each PSC cell sends less prohemocyte maintenance signal, something that is finally compensated by increased PSC cell number. One signal issued from the PSC and required to prevent premature differentiation of prohemocytes is Hh (7). We asked whether Hh expression in the PSC was dependent upon Col activity, using the HhF4-GFP reporter gene (33). Whereas HhF4-GFP expression was detected in both wt and col > tkv^{DN} PSCs, little or no expression was observed in col > coldsRNA conditions (Fig. 3 *C*–*E*′). This shows that maintenance of *col* expression during larval development is required to maintain Hh expression in the PSC. One other signature of PSC cells is the extension of numerous filopodia that can be visualized using mCD8-GFP and could possibly mediate signaling between the PSC and prohemocytes (7, 8, 33). Although observed in col > tkv^{DN} similarly to wt PSCs, filopodia were very reduced in col > coldsRNA PSCs (Fig. 3 *F*, *G*, and *H*), indicating that *col* expression in PSC cells is required for normal filopodia formation. These data establish that sustained *col* activity is required for the signaling properties of PSC cells.

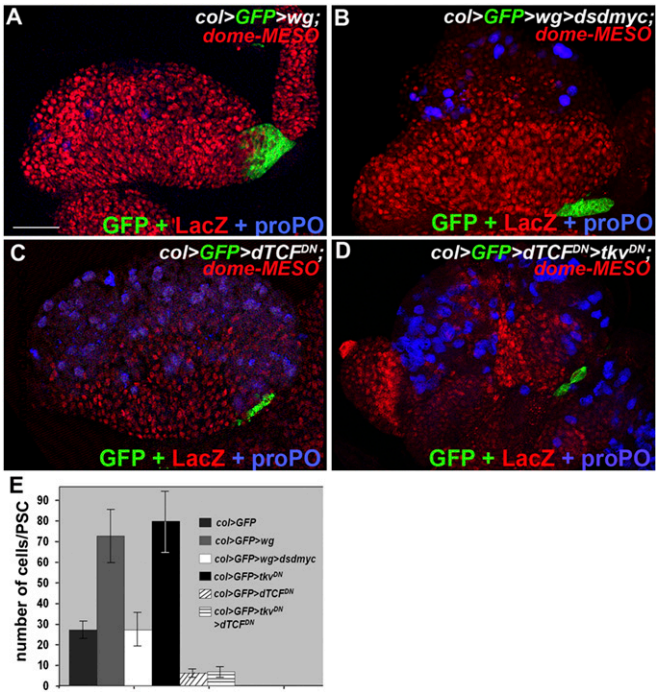

Fig. 5. Wingless signaling controls PSC cell number. (*A*) Increasing *wg* expression in the PSC (*col* > *GFP* > *wg*) leads to an increased number of PSC cells (green), expansion of the MZ (dome-MESO, red), and reduced crystal cell differentiation (proPO, blue). (*B*) PSC cell number and crystal cell differentiation return to wt when dmyc dsRNA is coexpressed with *wg*. (*C* and *D*) Blocking either Wg signaling (*col* > $dTCF^{DN}$) (*C*) or Wg plus Dpp signaling (*col*> $dTCF^{DN}$ > tkv^{DN}) (*D*) in the PSC results in a PSC containing six cells on average. (Scale bar: 80 μm *A*–*D*.) (*E*) Quantification of PSC cell numbers.

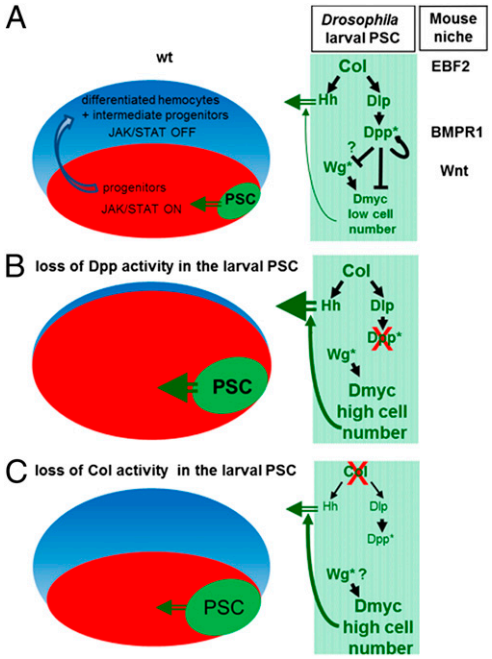

Fig. 6. Role of BMP and Wg signaling in the *Drosophila* PSC: parallels with the mouse HSC niche. (*A*–*C*) Schematic representation of *Drosophila* LGs (*Left*) and the interactions among Col, Dpp, and Wg signaling in the PSC (niche, green) (*Right*). (*A*) In wt LGs, signals issued from the PSC maintain Jak-Stat signaling in hemocyte progenitors (red) and control the balance between prohemocyte maintenance and hemocyte differentiation (intermediate progenitors and differentiated hemocytes, blue). Col activity in the PSC both controls the expression of Hh, one prohemocyte maintenance signal (7) and the niche size by restricting BMP signaling to PSC cells, via activation of Dlp. A paracrine/autocrine Dpp > dpp autoregulatory loop maintains a high level of BMP signaling and represses Dmyc in the PSC. Conversely, Wg signaling positively regulates Dmyc expression. Wg is epistatic to Dpp signaling in the PSC, but whether Dpp signaling only represses the Wg pathway or also acts in parallel to Wg in controlling *dmyc* expression remains an open question. *Represents the signaling pathway. The role of Dpp signaling in the PSC and roles of EBF2, BMPR1A, and Wnt in mouse osteoblasts (10, 44) highlight parallels between the *Drosophila* and mammalian hematopoietic niches. (*B*) Blocking Dpp activity in PSC cells leads to increased levels of Dmyc expression and increased number of cells. Because each PSC cell expresses normal levels of prohemocyte maintenance signals, the MZ receives more signal and more progenitors are maintained at the expense of differentiation. (*C*) Reducing Col expression in the larval PSC results in both down-regulation of Dlp expression and Dpp signaling and Hh expression, leading to an increase in the number of PSC cells, with each cell producing less Hh signal. The overall effect is restoring normal homeostasis in the LG.

However, and unlike the observation with Antp (7), *col* overexpression in the PSC (col > col) affected neither PSC cell numbers nor hemocyte homeostasis (Fig. S4), suggesting that Col does not act in the PSC in a dose-dependent manner. Altogether these data establish that Col activity in the niche controls hemocyte homeostasis via a BMP-dependent regulation of niche cell numbers and a BMP-independent regulation of the ability of PSC cells to signal to prohemocytes.

Repression of Dmyc Expression by BMP Signaling Is Crucial for Controlling Niche Size. *dmyc*/*diminutive*, which encodes the *Drosophila* ortholog of the vertebrate *myc* genes, plays a major role in controlling cell growth and proliferation in many tissues throughout development. In third-instar larvae, Dmyc is expressed at high levels in LG cells except in PSC cells (Fig. 4 *A*–*C*), correlating well with the low proliferation status of these cells. The increased levels of Dmyc observed in col > tkv^{DN} LGs indicate that *dmyc* expression is repressed by BMP signaling in the PSC (Fig. 4*C*). To assess the physiological role of this repression, we bypassed it, by placing *dmyc* expression under the control of *col* (col > dmyc, GFP). This resulted in a considerably oversized PSC containing hundreds of cells and accounting for as much as one-third of the total number of LG cells (Fig. 4*D*). Of note, the total LG size was not significantly changed, confirming that prohemocyte proliferation is independent of the PSC size. col > dmyc PSC cells express Antp and Col, and no or little hemocyte differentiation is observed in these LGs (Fig. 4*D*). This result strengthens the conclusion that too many niche cells result in an expansion of the prohemocyte pool at the expense of hemocyte differentiation. Reducing BMP signaling and *dmyc* expression at the same time restored the PSC size to 20 cells on average, which was similar to wt (Fig. 4 *F* and *G*), indicating that repression of *dmyc* expression by BMP signaling is essential to maintain the low number of PSC cells. Hemocyte differentiation was also restored, indicating that the absence of BMP signaling does not by itself affect the level of signaling from the PSC that is required for prohemocyte maintenance (Fig. 6) and that its major role in niche cells is to repress *dmyc* expression.

Opposite Regulations by Wg and Dpp Signaling Control the PSC Cell Number. The Wg pathway was shown to positively regulate the number of PSC cells (12). Wg signaling is mediated by nuclear translocation of dTCF (34). Consistent with the results obtained with a dominant-negative form of the Frizzled 2 receptor (12), expressing a dominant-negative form of dTCF ($dTCF^{DN}$) in the PSC leads to a reduction of the PSC cell number (Fig. 5 *C* and *E*) (33). Conversely, Wg overexpression increases the number of PSC cells to 70 on average (Fig. 5 *A* and *E*), a number similar to that observed upon blocking BMP signaling (Fig. 1 and Fig. S1). This underlines the opposite effects of these two signaling pathways in controlling the PSC size. Simultaneous overexpression of Wg and reduction of *dmyc* expression restores the wt PSC size (Fig. 5 *B*–*E*), indicating that the Wg pathway positively controls *dmyc* expression in the PSC. Together, these results show that Dmyc expression integrates opposite regulations by Wg and Dpp signaling to control the PSC cell number. To examine possible epistatic relations between Dpp and Wg signaling in the PSC, we simultaneously blocked both pathways (col > $dTCF^{DN}$ > tkv^{DN}). This led to a PSC containing six cells on average, which is similar to the number obtained when Wg signaling alone is inhibited (Fig. 5 *D* and *E*). This result indicates that Dpp signaling antagonizes Wg activity in the control of PSC cell numbers (Fig. 6).

Dlp can also regulate Wg movement, stability, and reception (35). Whether Dlp accumulation in the PSC specifically interconnects Wg and Dpp signaling in these cells is, thus, an interesting possibility. Unlike the observation in the PSC, in the *Drosophila* wing disk, Wg signaling represses *dmyc* expression via a double repression loop involving N signaling (36, 37). The molecular mechanisms by which the Wg and Dpp pathways control *dmyc* expression in PSC cells remain to be deciphered.

Parallels in the Molecular Cascades Controlling Hematopoiesis in Flies and Vertebrates. Osteoblasts are one major component of the niche in the mammalian bone marrow. Genetic studies in mice and ex vivo experiments have shown that several signaling pathways are involved in the communication between osteoblasts and HSCs (38–42). For instance, inactivation of β-catenin, the mediator of Wnt, results in reduced numbers of osteoblasts (43), reminiscent of the effect of removing Wg signaling in the *Drosophila* PSC (Fig. 6) (12). Likewise, a conditional knockout of the type 1A BMP receptor (BMPR1A) in osteoblasts results in an increase of the number of these cells and, as a consequence, an increased number of HSCs that are retained in the niche (10). Our finding that the BMP signaling pathway cell autonomously controls PSC cell proliferation, and as a consequence, the number of prohemocytes, thus brings to light a parallel between the *Drosophila* and mammalian hematopoietic niches (Fig. 6). Early B-cell factor (EBF)2, one Col mouse ortholog, has recently been shown to be expressed in osteoblastic cells and to regulate HSC maintenance. This is particularly noteworthy, given the key role of Col in controlling proliferation in the PSC and hemocyte homeostasis (9, 44). A similar Col-EBF > Dpp/BMP-signaling regulatory cascade could, thus, operate in controlling niche cell proliferation in the *Drosophila* LG and the mouse bone marrow. Whether the control of Myc expression in osteoblasts impacts on HSC quiescence and/or survival in the bone marrow is now an open question.

Materials and Methods

Imaging and Image Analysis. Images were collected with Leica SP2 and SP5 and Zeiss 710 confocal microscopes. All images shown are single confocal sections, except in Figs. 1 *K* and *L* and 2 *A* and *B*, which correspond to stacks (20 μm total depth). Mid-L3 larvae (96 h AEL) were used for LG analyses except in Fig. 5 and Fig. S4, for which mid-/late L3 (116 h AEL) larvae were used.

Mitotic Index Measurement. Anti-H3P staining was used to detect mitoses. The mitotic index in the PSC was measured by dividing the number of H3P-positive cells by the total number of col > GFP-labeled PSC cells. The total number of MZ and CZ cells was estimated as follows: the average surface of each LG was divided by the per-cell surface and multiplied by the number of cell layers in the LG, as determined by Z-series of SP2 confocal images (distance between each scan almost 1.5 μm). The LG surface was measured using the ImageJ (National Institutes of Health) software. The number of mitotic figures was counted and divided by the total number of LG cells (20 LGs per genotype). Statistical analysis was performed with Student *t* test.

Crystal Cell Number Quantification. Lymph glands were stained with proPO antibody (crystal cells) and Topro (nuclei). Confocal sections were 0.64 and 1.16 μm when using Leica SP5 and Zeiss 710 microscopes, respectively. The number of crystal cells and the volume (in micrometers cubed) of each anterior lobe were measured using Volocity 3D Image Analysis software (PerkinElmer). Crystal cell index corresponds to the number of crystal cells/(primary lobe volume/100,000). At least 24 anterior lobes were scored per genotype. Statistical analyses (Mann–Whitney nonparametric test) were performed using the GraphPad Prism 5 software.

ACKNOWLEDGMENTS. We thank C. Benassayag, K. Cadigan, G. Campbell, J. Casanova, J. Castelli-Gair Hombria, G. Pyrowolakis, R. Schulz, S. Thor, K. Wharton, and the Bloomington and Vienna Stock Center for fly strains; C. H. Heldin, A. Moore, T. Trenczek, and I. Ando for antibodies; E. Cau, J. L. Frendo, M. Meister, C. Monod, S. Plaza, and N. Vanzo for critical reading of the manuscript. We are grateful to B. Ronsin and A. Le Ru for assistance with confocal microscopy (Plateforme TRIO) and J. Favier and F. Luce for fly culture. We thank the reviewers for constructive remarks. Work in the laboratory of the authors is supported by Centre National de la Recherche Scientifique, University Toulouse III, Ministère de la Recherche (Agence Nationale de la Recherche Programme Blanc), Association pour la Recherche sur le Cancer, and Fondation pour la Recherche Médicale.

1. Krzemien J, Crozatier M, Vincent A (2010) Ontogeny of the Drosophila larval hematopoietic organ, hemocyte homeostasis and the dedicated cellular immune response to parasitism. *Int J Dev Biol* 54:1117–1125.
2. Lanot R, Zachary D, Holder F, Meister M (2001) Postembryonic hematopoiesis in Drosophila. *Dev Biol* 230:243–257.
3. Jung SH, Evans CJ, Uemura C, Banerjee U (2005) The Drosophila lymph gland as a developmental model of hematopoiesis. *Development* 132:2521–2533.
4. Lebestky T, Jung SH, Banerjee U (2003) A Serrate-expressing signaling center controls Drosophila hematopoiesis. *Genes Dev* 17:348–353.
5. Krzemien J, Oyallon J, Crozatier M, Vincent A (2010) Hematopoietic progenitors and hemocyte lineages in the Drosophila lymph gland. *Dev Biol* 346:310–319.
6. Crozatier M, Ubeda JM, Vincent A, Meister M (2004) Cellular immune response to parasitization in Drosophila requires the EBF orthologue collier. *PLoS Biol* 2:E196.
7. Mandal L, Martinez-Agosto JA, Evans CJ, Hartenstein V, Banerjee U (2007) A Hedgehog- and Antennapedia-dependent niche maintains Drosophila haematopoietic precursors. *Nature* 446:320–324.
8. Krzemień J, et al. (2007) Control of blood cell homeostasis in Drosophila larvae by the posterior signalling centre. *Nature* 446:325–328.
9. Crozatier M, Vincent A (2011) Drosophila: A model for studying genetic and molecular aspects of haematopoiesis and associated leukaemias. *Dis Model Mech* 4:439–445.
10. Zhang J, et al. (2003) Identification of the haematopoietic stem cell niche and control of the niche size. *Nature* 425:836–841.
11. Calvi LM, et al. (2003) Osteoblastic cells regulate the haematopoietic stem cell niche. *Nature* 425:841–846.
12. Sinenko SA, Mandal L, Martinez-Agosto JA, Banerjee U (2009) Dual role of wingless signaling in stem-like hematopoietic precursor maintenance in Drosophila. *Dev Cell* 16:756–763.
13. Leatherman JL, Dinardo S (2010) Germline self-renewal requires cyst stem cells and stat regulates niche adhesion in Drosophila testes. *Nat Cell Biol* 12:806–811.
14. Song X, et al. (2004) Bmp signals from niche cells directly repress transcription of a differentiation-promoting gene, bag of marbles, in germline stem cells in the Drosophila ovary. *Development* 131:1353–1364.
15. Xie T, Spradling AC (1998) Decapentaplegic is essential for the maintenance and division of germline stem cells in the Drosophila ovary. *Cell* 94:251–260.
16. Harris RE, Pargett M, Sutcliffe C, Umulis D, Ashe HL (2011) Brat promotes stem cell differentiation via control of a bistable switch that restricts BMP signaling. *Dev Cell* 20:72–83.
17. Goldman DC, et al. (2009) BMP4 regulates the hematopoietic stem cell niche. *Blood* 114:4393–4401.
18. Affolter M, Basler K (2007) The Decapentaplegic morphogen gradient: From pattern formation to growth regulation. *Nat Rev Genet* 8:663–674.
19. Raftery LA, Twombly V, Wharton K, Gelbart WM (1995) Genetic screens to identify elements of the decapentaplegic signaling pathway in Drosophila. *Genetics* 139: 241–254.
20. Tsuneizumi K, et al. (1997) Daughters against dpp modulates dpp organizing activity in Drosophila wing development. *Nature* 389:627–631.
21. Weiss A, et al. (2010) A conserved activation element in BMP signaling during Drosophila development. *Nat Struct Mol Biol* 17:69–76.
22. Sekelsky JJ, Newfeld SJ, Raftery LA, Chartoff EH, Gelbart WM (1995) Genetic characterization and cloning of mothers against dpp, a gene required for decapentaplegic function in Drosophila melanogaster. *Genetics* 139:1347–1358.
23. Frandsen JL, Gunn B, Muratoglu S, Fossett N, Newfeld SJ (2008) Salmonella pathogenesis reveals that BMP signaling regulates blood cell homeostasis and immune responses in Drosophila. *Proc Natl Acad Sci USA* 105:14952–14957.
24. Minakhina S, Steward R (2010) Hematopoietic stem cells in Drosophila. *Development* 137:27–31.
25. Belenkaya TY, et al. (2004) Drosophila Dpp morphogen movement is independent of dynamin-mediated endocytosis but regulated by the glypican members of heparan sulfate proteoglycans. *Cell* 119:231–244.
26. Lin X (2004) Functions of heparan sulfate proteoglycans in cell signaling during development. *Development* 131:6009–6021.
27. Kirkpatrick CA, Selleck SB (2007) Heparan sulfate proteoglycans at a glance. *J Cell Sci* 120:1829–1832.
28. Bornemann DJ, Duncan JE, Staatz W, Selleck S, Warrior R (2004) Abrogation of heparan sulfate synthesis in Drosophila disrupts the Wingless, Hedgehog and Decapentaplegic signaling pathways. *Development* 131:1927–1938.
29. Fujise M, et al. (2003) Dally regulates Dpp morphogen gradient formation in the Drosophila wing. *Development* 130:1515–1522.
30. Chen S, Wang S, Xie T (2011) Restricting self-renewal signals within the stem cell niche: Multiple levels of control. *Curr Opin Genet Dev* 21:684–689.
31. Crozatier M, Vincent A (2008) Control of multidendritic neuron differentiation in Drosophila: The role of Collier. *Dev Biol* 315:232–242.
32. Baumgardt M, Miguel-Aliaga I, Karlsson D, Ekman H, Thor S (2007) Specification of neuronal identities by feedforward combinatorial coding. *PLoS Biol* 5:e37.
33. Tokusumi Y, Tokusumi T, Stoller-Conrad J, Schulz RA (2010) Serpent, suppressor of hairless and U-shaped are crucial regulators of hedgehog niche expression and prohemocyte maintenance during Drosophila larval hematopoiesis. *Development* 137: 3561–3568.
34. Gordon MD, Nusse R (2006) Wnt signaling: Multiple pathways, multiple receptors, and multiple transcription factors. *J Biol Chem* 281:22429–22433.
35. Gallet A, Staccini-Lavenant L, Thérond PP (2008) Cellular trafficking of the glypican Dally-like is required for full-strength Hedgehog signaling and wingless transcytosis. *Dev Cell* 14:712–725.
36. Duman-Scheel M, Johnston LA, Du W (2004) Repression of dMyc expression by Wingless promotes Rbf-induced G1 arrest in the presumptive Drosophila wing margin. *Proc Natl Acad Sci USA* 101:3857–3862.
37. Herranz H, Pérez L, Martín FA, Milán M (2008) A Wingless and Notch double-repression mechanism regulates G1-S transition in the Drosophila wing. *EMBO J* 27: 1633–1645.
38. Kiel MJ, Morrison SJ (2008) Uncertainty in the niches that maintain haematopoietic stem cells. *Nat Rev Immunol* 8:290–301.
39. Wilson A, et al. (2008) Hematopoietic stem cells reversibly switch from dormancy to self-renewal during homeostasis and repair. *Cell* 135:1118–1129.
40. Garrett RW, Emerson SG (2009) Bone and blood vessels: The hard and the soft of hematopoietic stem cell niches. *Cell Stem Cell* 4:503–506.
41. Li L, Clevers H (2010) Coexistence of quiescent and active adult stem cells in mammals. *Science* 327:542–545.
42. Trumpp A, Essers M, Wilson A (2010) Awakening dormant haematopoietic stem cells. *Nat Rev Immunol* 10:201–209.
43. Nemeth MJ, Mak KK, Yang Y, Bodine DM (2009) beta-Catenin expression in the bone marrow microenvironment is required for long-term maintenance of primitive hematopoietic cells. *Stem Cells* 27:1109–1119.
44. Kieslinger M, Hiechinger S, Dobreva G, Consalez GG, Grosschedl R (2010) Early B cell factor 2 regulates hematopoietic stem cell homeostasis in a cell-nonautonomous manner. *Cell Stem Cell* 7:496–507.
45. Enriquez J, et al. (2010) Multi-step control of muscle diversity by Hox proteins in the Drosophila embryo. *Development* 137:457–466.